Chapter 67
Estimation of Electric Drive Vehicle Sideslip Angle Based on EKF

Guibing Yang, Chunguang Liu and Dingzhe Qin

Abstract The sideslip angle is the most crucial state variable in the stability control system for vehicles, particularly in the electric drive vehicle field. But recently, there is no other way that could obtain the sideslip angle directly with low cost. Due to the characteristic of strongly nonlinear vehicle system, this paper discusses how to evaluate the sideslip angle with the extended Kalman filter (EKF) algorithm and build both double-track kinematics model and tire model, and then, we proposed the conception of nonlinear state space description and analyzed the result with a simulation method ultimately.

Keywords Electric drive · EKF · Sideslip angle · Vehicle dynamics

67.1 Introduction

Recently, most of researchers focus on the study of vehicle state and parameter estimation, and clearly, the accuracy of state and parameter estimation affects the control performance of vehicle control system.

The sideslip angle is the most crucial state variable in the stability control system for vehicles. At present, there are two kinds of method for achieving the sideslip angle [1–4]: The first one depends on the GPS sensor signal for detection, and the other one employs estimated method which adopts the principle of kinematics and the kinetic. The former is not suitable for general usage because of high cost; therefore, the latter becomes the majority of the recent studies.

G. Yang (✉) · C. Liu
Department of Control Engineering, The Academy of Armored Force Engineering,
No. 21 Du jia kan, Feng Tai, Beijing, China
e-mail: 609794121@qq.com

D. Qin
Department of Training, The Academy of Armored Force Engineering,
No. 21 Du jia kan, Feng Tai, Beijing, China
e-mail: qindingzhe@163.com

L. Jia et al. (eds.), *Proceedings of the 2015 International Conference on Electrical and Information Technologies for Rail Transportation*,
Lecture Notes in Electrical Engineering 377, DOI 10.1007/978-3-662-49367-0_67

Taking eight-wheel independent drive vehicle as research object, this paper develops a double-track kinematics model, makes real-time estimation for sideslip angle by using EKF algorithm, and then verifies the estimated result with real-time simulation method.

67.2 Modeling of Dynamics

67.2.1 Vehicle Dynamics Model

Assuming that the longitudinal speed makes no changes on the moment of vehicle turning, without taking into consideration longitudinal acceleration and deceleration, we can develop a double-track kinematics model, which contains transverse movement and yawing motion, as shown in Fig. 67.1.

Double-track kinematics model of vehicle with 2 DOF is expressed as follows:

$$\begin{aligned} a_y = \frac{1}{m}(&F_{y11}\cos\delta_{11} + F_{x11}\sin\delta_{11} + F_{y12}\cos\delta_{12} + F_{x12}\sin\delta_{12} + F_{y21}\cos\delta_{21} \\ &+ F_{x21}\sin\delta_{21} + F_{y22}\cos\delta_{22} + F_{x22}\sin\delta_{22} + F_{y31} + F_{y32} + F_{y41} + F_{y42}) \end{aligned} \quad (67.1)$$

$$\begin{aligned} a_x = \frac{1}{m}(&-F_{y11}\sin\delta_{11} + F_{x11}\cos\delta_{11} - F_{y12}\sin\delta_{2} + F_{x12}\cos\delta_{12} - F_{y21}\sin\delta_{21} \\ &+ F_{x21}\cos\delta_{21} - F_{y22}\sin\delta_{22} + F_{x22}\sin\delta_{22} + F_{x31} + F_{x32} + F_{x41} + F_{x42}) \end{aligned} \quad (67.2)$$

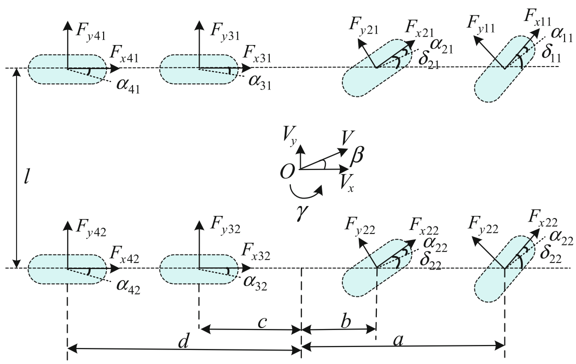

Fig. 67.1 Double-track kinematics model of vehicle with 2 DOF

$$\dot{\gamma} = \frac{1}{I_z}[a(F_{y11}\cos\delta_{11} + F_{x11}\sin\delta_{11} + F_{y12}\cos\delta_{12} + F_{x12}\sin\delta_{12}) + b(F_{y21}\cos\delta_{21} + F_{x21}\sin\delta_{21} + F_{y22}\cos\delta_{22} + F_{x22}\sin\delta_{22}) - c(F_{y31} + F_{y32}) - d(F_{y41} + F_{y42}) + \frac{l}{2}(F_{x12}\cos\delta_{12} + F_{x22}\cos\delta_{22} + F_{x32} + F_{x42} - F_{x11}\cos\delta_{11} - F_{x21}\cos\delta_{21} - F_{x31} - F_{x41})] \tag{67.3}$$

$$\dot{\beta} = \frac{1}{mV}[F_{y11}\cos(\beta - \delta_{11}) + F_{y12}\cos(\beta - \delta_{12}) + F_{y21}\cos(\beta - \delta_{21}) + F_{y22}\cos(\beta - \delta_{22}) - F_{x11}\sin(\beta - \delta_{11}) - F_{x12}\sin(\beta - \delta_{12}) - F_{x21}\sin(\beta - \delta_{21}) - F_{x22}\sin(\beta - \delta_{22}) + (F_{y31} + F_{y32} + F_{y41} + F_{y42})\cos\beta - (F_{x31} + F_{x32} + F_{x41} + F_{x42})\sin\beta] - \gamma \tag{67.4}$$

$$\dot{V} = \frac{1}{m}[F_{y11}\sin(\beta - \delta_{11}) + F_{y12}\sin(\beta - \delta_{12}) + F_{y21}\sin(\beta - \delta_{21}) + F_{y22}\sin(\beta - \delta_{22}) + F_{x11}\cos(\beta - \delta_{11}) + F_{x12}\cos(\beta - \delta_{12}) + F_{x21}\cos(\beta - \delta_{21}) + F_{x22}\cos(\beta - \delta_{22}) + (F_{y31} + F_{y32} + F_{y41} + F_{y42})\sin\beta + (F_{x31} + F_{x32} + F_{x41} + F_{x42})\cos\beta] \tag{67.5}$$

where F_{xij} is the tire longitudinal forces, F_{yij} is the lateral tire forces, m is the vehicle mass, and I_z is the yaw moment of inertia. The forward velocity V, steering angle δ_{ij}, yaw rate γ, and the vehicle slip angle β are then used to calculate the tire slip angles α_{ij}, where

$$\begin{cases} \alpha_1 = \delta_1 - (\beta + a\gamma/V_x) \\ \alpha_2 = \delta_2 - (\beta + a\gamma/V_x) \\ \alpha_3 = \delta_3 - (\beta + b\gamma/V_x) \\ \alpha_4 = \delta_4 - (\beta + b\gamma/V_x) \\ \alpha_5 = \alpha_6 = -\beta + c\gamma/V_x \\ \alpha_7 = \alpha_8 = -\beta + d\gamma/V_x \end{cases} \tag{67.6}$$

67.2.2 Tire Model

The Dugoff tire model is chosen for our study. It is expressed as follows:

$$\begin{cases} F_{yij} = -C_{\alpha ij} \tan \alpha_{ij} f(\lambda) \\ f(\lambda) = \begin{cases} (2-\lambda)\lambda, & \text{if } \lambda < 1 \\ 1, & \text{if } \lambda \geq 1 \end{cases} \\ \lambda = \frac{\mu_{\max} F_{zij}}{2C_{\alpha ij} \left| \tan \alpha_{ij} \right|} \end{cases} \tag{67.7}$$

The model describes a tire model with the characteristic of nonlinear lateral force [5] and applies less parameter, where $C_{\alpha ij}$ is the lateral stiffness and F_{zij} is the normal load on the tire.

When the vehicle sideslip angle changes, a lateral tire force is created with a time lag. This transient behavior of tires can be formulated using a relaxation length δ [6], and the dynamic lateral forces can be written as follows:

$$\dot{F}_{yij} = \frac{V}{\delta_{ij}} (-F_{yij} + \bar{F}_{yij}) \tag{67.8}$$

where $\bar{F}_{yij}$ is calculated from the quasi-static Dugoff tire model.

67.3 Stochastic State Space Representation

The nonlinear stochastic state space representation of the system described in the previous section is given as follows:

$$\begin{cases} \dot{X}(t) = f(X(t), U(t)) + w(t) \\ Y(t) = h(X(t), U(t)) + v(t) \end{cases} \tag{67.9}$$

The input vector U comprises the steering angle and the normal forces

$$\begin{aligned} U &= [\delta_{11}, \delta_{12}, \delta_{21}, \delta_{22}, F_{z11}, F_{z12}, \ldots, F_{z42}]^T \\ &= [u_1, u_2, u_3, u_4, u_5, u_6, \ldots, u_{12}]^T \end{aligned} \tag{67.10}$$

The measure vector Y comprises yaw rate, vehicle velocity, and longitudinal and lateral accelerations

$$Y = [\gamma, V, a_x, a_y]^T = [y_1, y_2, y_3, y_4]^T \tag{67.11}$$

The state vector X comprises yaw rate, vehicle velocity, sideslip angle at the COG, lateral forces, and longitudinal tire forces.

$$
\begin{aligned}
X &= [\gamma, V, \beta, F_{y11}, F_{y12}, \ldots, F_{y42}, F_{x11}, F_{x12}, \ldots, F_{x42}]^T \\
&= [x_1, x_2, x_3, x_4, x_5, \ldots, x_{12}, x_{13}, \ldots, x_{19}]^T
\end{aligned}
\tag{67.12}
$$

The process and measurement noise vectors ω and v, respectively, are assumed to be white, zero mean, and uncorrelated.

The particular nonlinear function $f(.)$ of the state equations is given by

$$
\begin{cases}
f_1 = \frac{1}{I_z}[a(x_4 \cos\mu_1 + x_{12}\sin\mu_1 + x_5\cos\delta_{12}\mu_2 + x_{13}\sin\mu_2) \\
\quad + b(x_6\cos\mu_3 + x_{14}\sin\mu_3 + x_7\cos\mu_4 + x_{15}\sin\mu_4) \\
\quad - c(x_8 + x_9) - d(x_{10} + x_{11}) + \frac{l}{2}(x_{13}\cos\mu_2 + x_{15}\cos\mu_4 \\
\quad + x_{17} + x_{19} - x_{12}\cos\mu_1 - x_{14}\cos\mu_3 - x_{16} - x_{18})]; \\
f_2 = \frac{1}{m}[x_4\sin(x_3 - \mu_1) + x_5\sin(x_3 - \mu_2) + x_6\sin(x_3 - \mu_3) \\
\quad + x_7\sin(x_3 - \mu_4) + x_{12}\cos(x_3 - \mu_1) + x_{13}\cos(x_3 - \mu_2) \\
\quad + x_{14}\cos(x_3 - \mu_3) + x_{15}\cos(x_3 - \mu_4) + (x_8 + x_9 + x_{10} + x_{11}) \\
\quad \sin x_3 + (x_{16} + x_{17} + x_{18} + x_{19})\cos x_3]; \\
f_3 = \frac{1}{mx_2}[x_4\cos(x_3 - \mu_1) + x_5\cos(x_3 - \mu_2) + x_6\cos(x_3 - \mu_3) \\
\quad + x_7\cos(x_3 - \mu_4) + x_{12}\sin(x_3 - \mu_1) + x_{13}\sin(x_3 - \mu_2) \\
\quad + x_{14}\sin(x_3 - \mu_3) + x_{15}\sin(x_3 - \mu_4) + (x_8 + x_9 + x_{10} + x_{11}) \\
\quad \cos x_3 + (x_{16} + x_{17} + x_{18} + x_{19})\sin x_3] - x_1; \\
f_4 = \frac{x_2}{\sigma_{11}}(-x_4 + \bar{F}_{y11}(\alpha_{11}, \mu_5)); \\
f_5 = \frac{x_2}{\sigma_{12}}(-x_5 + \bar{F}_{y12}(\alpha_{12}, \mu_6)); \\
\quad \ldots \\
f_{11} = \frac{x_2}{\sigma_{42}}(-x_{11} + \bar{F}_{y42}(\alpha_{42}, \mu_{12})); \\
f_{12} = 0; \\
\quad \ldots \\
f_{19} = 0
\end{cases}
\tag{67.13}
$$

The observation function $h(.)$ is given by

$$
\begin{cases}
h_1 = x_1; \\
h_2 = x_2; \\
h_3 = \frac{1}{m}(-x_4\sin u_1 + x_{12}\cos u_1 - x_5\sin u_2 + x_{13}\cos u_2 \\
\quad - x_6\sin u_3 + x_{14}\cos u_3 - x_7\sin u_4 + x_{15}\sin u_4 \\
\quad + x_{16} + x_{17} + x_{18} + x_{19}) \\
h_4 = \frac{1}{m}(x_4\cos u_1 + x_{12}\sin u_1 + x_5\cos u_2 + x_{13}\sin u_2 \\
\quad + x_6\cos u_3 + x_{14}\sin u_3 + x_7\cos u_4 + x_{15}\sin u_4 \\
\quad + x_8 + x_9 + x_{10} + x_{11})
\end{cases}
\tag{67.14}
$$

67.4 EKF Algorithm

The first-order EKF is presented as follows.

(a) **Initialization**:
The initial state and the initial covariance are determined by

$$\begin{aligned} \bar{X}_0 &= E[X_0], \\ p_0 &= E[(X_0 - \bar{X}_0)(X_0 - \bar{X}_0)^T] \end{aligned} \tag{67.15}$$

(b) **Time Update**:
The prediction of the state is given by

$$\bar{X}_{k|k-1} = f(\bar{X}_{k-1|k-1}, U_k) \tag{67.16}$$

The predicted covariance is computed as

$$P_{k|k-1} = AP_{k-1|k-1}A^T + Q \tag{67.17}$$

(c) **Measurement Update**:
The filter gain is calculated by

$$K_k = P_{k|k-1}H^T[HP_{k|k-1}H^T + R]^{-1} \tag{67.18}$$

The state estimation is determined by

$$\bar{X}_{k|k} = \bar{X}_{k|k-1} + K_k[Y_k - h(\bar{X}_{k|k-1})] \tag{67.19}$$

The estimated covariance is

$$P_{k|k} = [I - K_k H]P_{k|k-1} \tag{67.20}$$

A_k and H_k are the process and measurement Jacobians at step k of the non-linear equations around the estimated states.

$$\begin{cases} A_k = \frac{\partial f(\bar{X}_{k-1|k-1}, U_k, 0)}{\partial X} \\ H_k = \frac{\partial h(\bar{X}_{k|k-1}, 0)}{\partial X} \end{cases} \tag{67.21}$$

67.5 Simulation

(a) High-speed hunting driving in good road condition
(b) Low-speed hunting driving in good road condition
(c) Hunting driving in low-friction road condition

In Figs. 67.2, 67.3 and 67.4, they show that the estimated value of sideslip angle is basically in accordance with that of simulation under the three typical motions.

Fig. 67.2 Sideslip angle

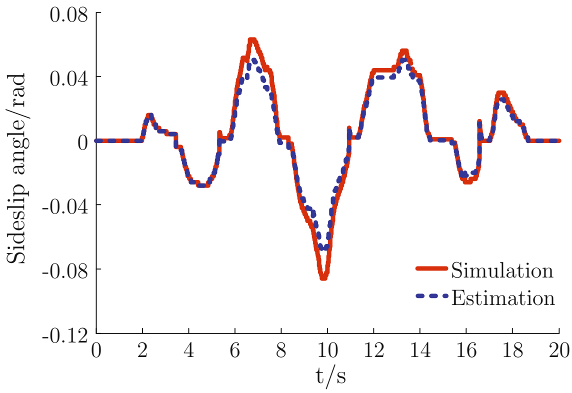

Fig. 67.3 Sideslip angle

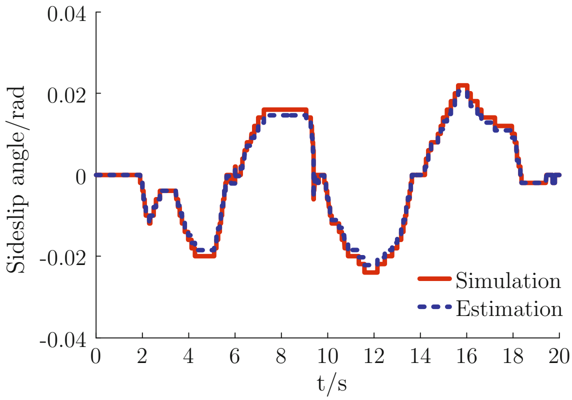

Fig. 67.4 Sideslip angle

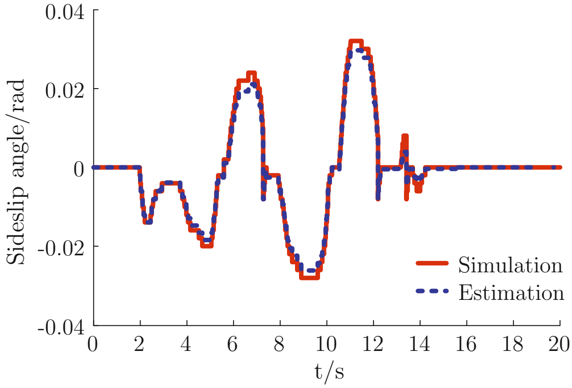

67.6 Conclusion

This paper applies EKF filter algorithm for evaluating the sideslip angle of vehicles, chooses Dugoff tire model which is based on the double-track kinematics model, and then extends a nonlinear state space for the filter estimation. The simulation result shows that the filter method using EFK would have better performance for vehicle sideslip angle.

References

1. Li L, Wang F, Zhou Q (2006) Integrated longitudinal and lateral tire/road friction modeling and monitoring for vehicle motion control. IEEE Trans Intell Transp Syst 7(1):1–19 (in Chinese)
2. Manning WJ, Crolla DA (2007) A review of yaw rate and sideslip controllers for passenger vehicles. Trans Inst Meas Control 29(2):117–135
3. Wenjie G, Mei H, Weige Z (2013) Economic operation analysis of the electric vehicle charging station. Trans China Electrotechnical Soc 28(2):15–21 (in Chinese)
4. Shino M, Nagai M (2003) Independent wheel torque control of small-scale electric vehicle for handling and stability improvement. JSAE Rev 24(4):449–456
5. Pacejka HB (2002) Tyre and vehicle dynamics. Elsevier, New York
6. Rajamani R (2005) Vehicle dynamics and control. Springer, Berlin